Taiz University Research Journal, Volume 34 jan2023 ISSN: 2985-7848
Taiz University
2nd ICTSA -2022 Proceedings
17 -19 Dec, 2022, Taiz University, Taiz, Republic of Yemen.

Structural and Optical properties of Cd SeGe amorphous films

A. M. Al-Rebati[1] , Ebrahim M. Abuassag[1], M. A. Dabban[2] Mohammed M. H. Al-Awadhi[3]

[1]Physics Department, Faculty of Science and Education, Saba Region University, Marib, Yemen

[2]Physics Department, Faculty of Science, University of Aden, Aden, Yemen

[3]Chemistry Department, Faculty of Science and Education, Saba Region University, Marib, Yemen

* **Corresponding author:** *alribaty@usr.*ac

Abstract:

Thin films of $Cd_{10}Se_{75}Ge_{15}$ were prepared by the conventional thermal evaporation technique on glass substrate. The chemical composition of the films has been checked using energy dispersive X-ray spectroscopy (EDX). X-ray diffraction (XRD) measurements have shown that all investigated compositions in powder and thin film form have amorphous nature. Transmittance measurements in the wavelength range (350-2500nm) were used to calculate the refractive index n and the absorption index k using Swanepole's method. The analysis of the optical absorption data revealed that the optical band gap E_g was indirect transitions. The optical dispersion parameters E_o and E_d were determined according to Wemple and Didomenico method. The optical constants such as optical band gap E_g^{opt}, complex dielectric constant and dissipation factor $\tan\delta$ were determined.

Keywords: Cd Se Ge_thin films; optical constants; dispersion parameters

1. Introduction

Chalcogenide glassy semiconductors have several useful properties that can be employed in various solid state devices.They show a continuous change in physical properties with change in chemical composition [1]. They have also found applications in the fabrication of inexpensive solar cells [2], and as reversible phase change optical recorders [3]. So it is important to study their optical and electronic properties. The addition of an impurity has a pronounced effect on the conduction mechanism and the structure of the amorphous glass. This effect is widely different for different impurities [4]. Impurity effects in chalcogenide glasses have a great importance in fabrication of glassy semiconductors. These impurities are added to these glasses to modify thermal, mechanical, electrical and optical properties and enable the development of new materials with high quality for device industry. Different factors affect the role of impurity atoms in chalcogenide glasses, which is related to the composition of the glasses, the chemical nature of impurity and the value of impurity concentration. Several studies [5-8] have been made and reported the impurity effect in various chalcogenide glasses. The common feature of these glasses is the presence of localized states in the mobility gap as a result of the absence of long-range order as well as various inherent defects. The addition of metals such as Cd to Se-Ge chalcogenide glasses is generally accompanied by a marked change in their structural and physical properties [9-14]. The aim of this work was thus to calculate the optical parameters of evaporated $Cd_{10}Se_{75}Ge_{15}$ thin films and to investigate the relation to their thickness.

2. Experimental details.

Glassy alloys of $Cd_{10}Se_{75}Ge_{15}$ were synthesized by quenching technique.The elementary constituents of each composition of purity 99.999% were weighed in accordance with their atomic percentage and loaded in a silica tube, which was then sealed under vacuum (10^{-6} mbar). The content of each tube was heated gradually in an oscillatory furnace to 280 ^{o}C ($\approx$ m.p of Se) and kept constant for 2 h. It was raised to 321 ^{o}C ($\approx$ m.p of Cd and kept constant for 2 hrs. Finally it was raised to 980 ^{o}C ($\approx$m.p of Ge) and kept constant for 20 h. Long times of synthesis and oscillation of the tube are necessary for the homogeneity of the synthesized compositions. The tube is then quenched in icy water to obtain the compositions in the glassy state. Thin films of the investigated compositions were obtained from bulk samples by a thermal evaporation technique under vacuum on glass substrates for structural and optical measurements. The substrates was fixed onto a rotatable holder (up to 240 rpm) to obtain homogeneous deposited films at a distance of 25 cm above the evaporator. The thickness of film samples was measured during deposition using a thickness monitor (FTM2). The chemical composition of the investigated samples was checked by energy dispersive X-ray analysis (EDX) using scanning electron microscope (Joel JSM 5400). The structural identification of the investigated compositions

in powder and thin film forms were confirmed by both X-ray diffraction (XRD) and differential thermal analysis (DTA). Transmittance $T(\lambda)$ and reflectance $R(\lambda)$ at normal incidence were measured using a double beam spectrophotometer (JASCO Corp., V-570, Rev. 1.00.) with unpolarized light at normal incidence in the wave length range 350-2500 nm.

3. 3- Results and discussion.

3.1. Structural identification of $Cd_{10}Se_{75}Ge_{15}$film samples.
3.1.1. Energy dispersive X-ray spectroscopy.

Composition of the investigated films was checked using energy dispersive X-ray spectroscopy. The obtained percentages of their constituent elements are $Cd_{10}Se_{75}Ge_{15}$. Moreover EDX analysis indicates the absence of strange elements in the studied composition and illustrated in Fig.(1)a.

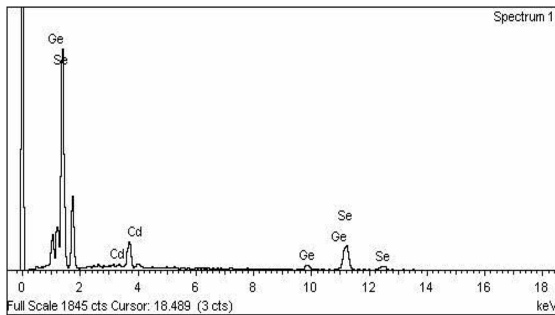

Fig.(1)a *Energy dispersive X-ray (EDX)- of $Cd_{10}Se_{75}Ge_{15}$ composition.*

3.1.2. X-ray diffraction characterization.

X-ray diffraction patterns for the investigated compositions in powder and thin film forms are illustrated in Fig.(1)b. No line matching is observed in this figure. The absence of the lines in the measured pattern indicates the formation of this composition have an amorphous structure.

3.1.3. Differential thermal analysis.

Differential thermal analysis was carried out at a constant heating rate (10 ^oC/min.). The obtained glass transition temperature, T_g for the studied samples is 130 ^oC.

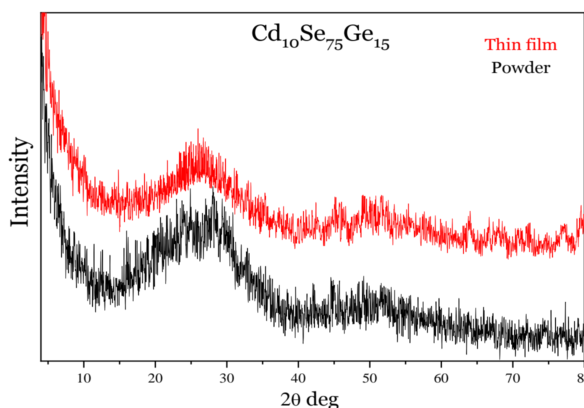

Fig.(1)b *X-ray diffraction patterns of $Cd_{10}Se_{75}Ge_{15}$ in powder and thin film form*

3.2. Optical properties of $Cd_{10}Se_{75}Ge_{15}$ thin films.

The study of the optical absorption of the investigated compositions, particularly the absorption edge has proved to be very important to study the electronic structure of these materials. The spectral distribution of the refractive index n, the absorption index k and the absorption coefficient α were determined using Swanepole's method [15]. The analysis of the absorption coefficient was carried out to obtain the optical energy gap E_g^{opt}. Analysis of the refractive index n with the help of the absorption index k was carried out to obtain the real and imaginary parts of the complex dielectric constant (ε_1 and ε_2), the optical dispersion parameters E_d, $E_o$and the dissipation factor $\tan\delta$.

3.2.1. *The spectral distribution of the transmittance and reflectance.*

The spectral distribution of transmittance T(λ) and reflectance R(λ) of the deposited films were measured at room temperature using unpolarized light at normal incidence in the wavelength range (350 - 2500 nm). Fig.(2) show the spectral distribution curves of transmittance T(λ) and reflectance R(λ) for the examined $Cd_{10}Se_{75}Ge_{15}$films at the thickness 512 nm. It is clear from this figure that at the larger wavelength region films become transparent, T+R=1 and no light is absorbed (k=0).

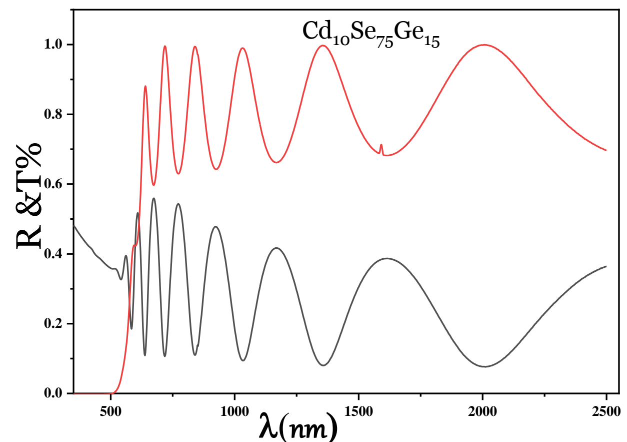

Fig.(2)a *Spectral distribution of transmittance T(λ) and reflectance R(λ) for $Cd_{10}Se_{75}Ge_{15}$amorphous film with thickness 512nm.*

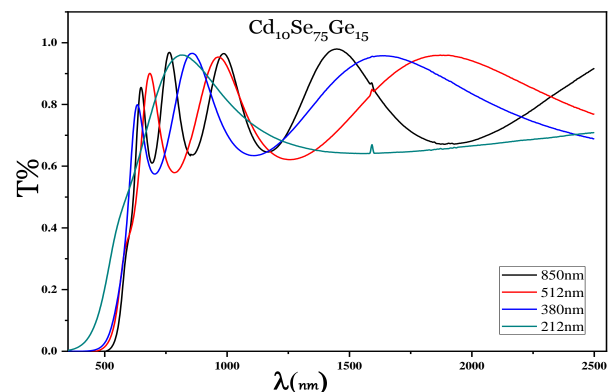

Fig.(2)b Spectral distribution of transmittance T(λ) for $Cd_{10}Se_{75}Ge_{15}$amorphous film with different thicknesses.

3.2.2. The dispersion curves of refractive index (n) and absorption index (k).

The refractive index *n* and absorption index *k* for the examined compositions were computed from the obtained $T(\lambda)$ using Swanepoel's method [15]. The spectral distribution of *n* and *k* for all investigated compositions are shown in Fig.(3) and (4), respectively

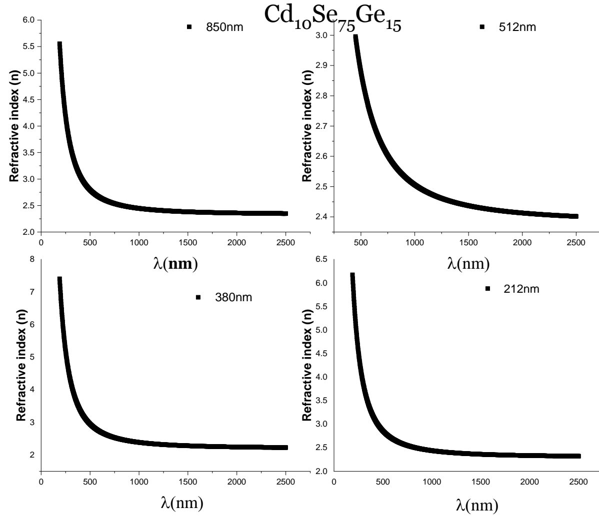

Fig.(3) Spectral dependence of the refractive index n for $Cd_{10}Se_{75}Ge_{15}$ thin films.

3.2.3. The spectral distribution of the absorption coefficient (α).

The spectral distribution of the absorption coefficient of a semiconductor near the fundamental edge is of great importance for the investigation of the allowed transitions, as well as, the energy band structure.The absorption coefficient (α) of the investigated films was calculated by two procedures, the first from the relation $\alpha = 4\pi k/\lambda$, which depends on values of *k,* calculated using Swanepoel's method. The second procedure is the calculation of α from the formula [16] $\alpha = (1/t).\ln((1-R)^2/T)$ where t is the film thickness. The obtained values of α from both procedures have approximately the same magnitude. A plot of $\log\alpha$ as a function of photon energy ($h\nu$) of the incident photons for the investigated thin films is illustrated in Fig. (5). Each curve of this figure can be divided into two regions[17].

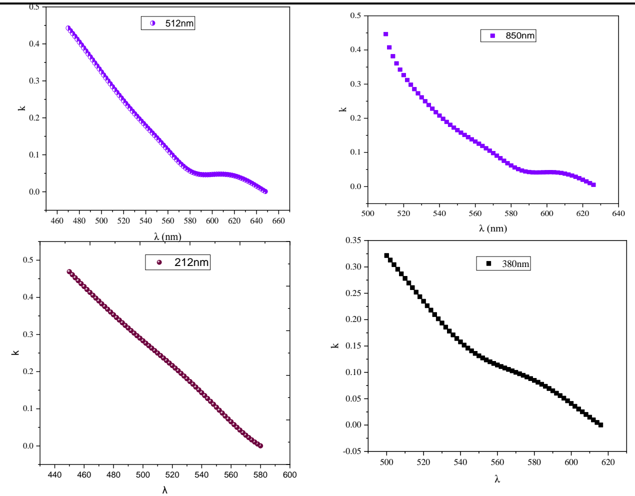

Fig.(4) Spectral dependence of the absorption index k for $Cd_{10}Se_{75}Ge_{15}$ thin films..

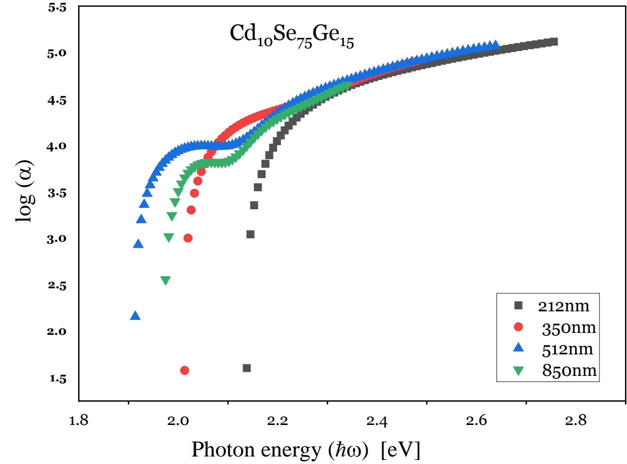

Fig.(5) *Plots of $\log\alpha$ as a function of photon energy $h\nu$ for $Cd_{10}Se_{75}Ge_{15}$amorphous films.*

(i) ***The first region***; for the higher values of the absorption coefficient, $\alpha(\nu) \geq 10^4$ cm^{-1}. This corresponds to transitions between extended states in both valence and conduction bands, where the power law behavior of Tauc[17],

$$\alpha h\nu = A(h\nu - E_g^{opt})^r \qquad (1)$$

is valid. The edge width parameter *A* representing the film quality, E_g^{opt} is the optical energy gap of the material and *r* is a number characterizing the type of the optical transition process. The parameter *r* has the value 1/2 for the direct allowed transition and has the value 2 for the indirect allowed transition. The usual method for the determination of the value of E_g^{opt} involves plotting a graph of $(\alpha h\nu)^{1/r}$ against $h\nu$. The relations $(\alpha h\nu)^{1/2} = f(h\nu)$ is plotted in Fig.(6) for amorphous $Cd_{10}Se_{75}Ge_{15}$films. This figure shows that $(\alpha h\nu)^{1/2} = f(h\nu)$ is linear relationship for all the investigated samples, indicating the existence of the indirect allowed transitions. Extrapolation of the linear parts dependence of $(\alpha h\nu)^{1/2} = A(h\nu - E_g^{opt})$ to the zero absorption with the photon energy axis yields the corresponding band width E_g^{opt}. The edge width parameter *A* can be calculated from the slopes of these linear parts for the investigated compositions. The obtained values of E_g^{opt} and *A*

are given in Table 1.

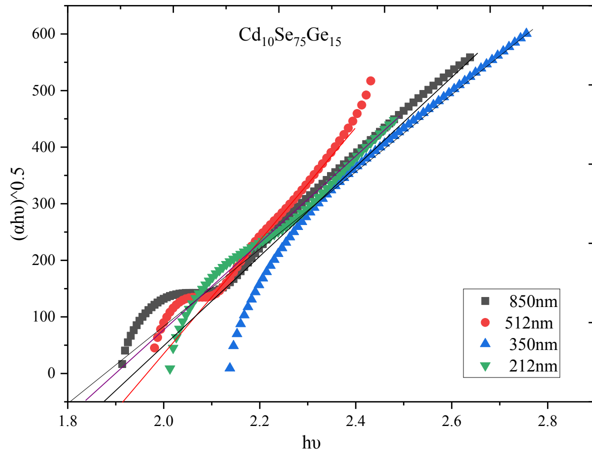

Fig.(6) Dependence of $(\alpha h\nu)^{1/2}$ on the photon energy $h\nu$ for $Cd_{10}Se_{75}Ge_{15}$amorphous films.

(ii) *The second region* of the absorption edge is for the lower values of the absorption coefficient, that is for $\alpha(\nu) < 10^4$ cm^{-1}, where the absorption at lower photon energy usually follows the Urbach rule[18] i.e.

$$\alpha(\nu) = \alpha_o \exp(h\nu/E_e) \quad (2)$$

where (α_o) is a constant and (E_e) is Urbach energy which is interpreted as the width of the tails of localized states in the band gap and in general represents the degree of disorder in an amorphous semiconductor [19], the absorption in this region is due to transitions between extended states in one band and localized states in the exponential tail of the other band [20].

From plotting $\log\alpha$ as a function of $h\nu$, shown in Fig.(5), values of E_e as a function of thickness can be calculated and given in Table 1.

Table 1. *Optical constants the edge width parameter A, the optical energy gap E_g^{opt} and Urbach energy(E_e) of $Cd_{10}Se_{75}Ge_{15}$ amorphous films with different thicknesses.*

Composition	E_g^{opt} (eV)	A, cm^{-1}.eV^{-1}	E_e (eV)
850nm	1.99	3.33E-07	0.12
512nm	1.9	3.44E-14	0.0581
380nm	1.88	1.71E-15	0.053
212nm	1.78	2.32E-16	0.05

It is clear form this table energy gap and Urbach energy E_e decrease with decreases films thickness. Also, the observed change of energy gap for all thicknesses can be explained using the density of states model in amorphous solids proposed by Mott and Davis [21]. According to this, the width of the localized states near the mobility edges depends on the degree of disorder and defects present in the amorphous structure. In particular, it is known that the unsaturated bonds are responsible for the formation of some defects in amorphous solids. Such defects produce localized states in the band structure.

3.2.4. Dispersion energy parameters.

Wemple and Didomenico [22,23] used a single-oscillator d escription of the frequency-dependent dielectric constant to define a "dispersion energy" parameters E_d and E_o. The refractive index dispersion of the studied samples can be f itted by Wemple and Didomenico model. The dispersion p lays an important role in the research for optical materials, because it is a significant factor in optical communication and in designing devices for spectral dispersion. Althoug h these rules are quite different in details, one common fe ature is the over-whelming evidence that both crystal struc ture and ionicity influence the refractive-index behavior of solids in ways that can be simply described [24]. The rel ation between the refractive index n, and the single oscil lator strength below the band gap is given by the expressi on [22,23]:

$$n^2 = 1 + \frac{E_o E_d}{E_o^2 - (h\nu)^2}, \quad (3)$$

where E_d and E_o are single oscillator constants, E_o the e nergy of the effective dispersion oscillator, E_d the so-calle d dispersion energy, which measures the average strength of interband optical transitions. Fig. (8) illustrates the plott ing of $(n^2-1)^{-1}$ versus $(h\nu)^2$ for the investigated films, which yields a straight line for normal behavior having th e slope $(E_oE_d)^{-1}$ and the intercept with the vertical axis is E_o/E_d. The obtained curves showed a positive curvature d eviation from linearity at longer wavelength, which is usu ally observed due to the negative contribution of lattice vi brations on the refractive index [23]. The obtained values of the parameters E_o and E_d are given in Table (2).

Table 2. *The parameters **energy of the effective dispersion oscillator** E_o, dispersion energy E_d and Wemple and Didomenico optical energy E_{opt}^{WD} for $Cd_{10}Se_{75}Ge_{15}$amorphous films.*

Composition	E_o, eV	E_d, eV	E_{opt}^{WD}, eV	n_s	$n_s^4 E_{opt}^{WD}$~60
212nm	2.93	11.3	1.465	2.204	35
380nm	3.42	14.7	1.71	2.302	47
512nm	3.68	17	1.843	2.32	59.54
850nm	3.94	17.73	1.9723	2.344	59.59

The obtained values of E_o and E_d for the studied comp ositions have slight differences with those obtained before [25], this may be due to the difference in the structure pr operties and the impurities of the investigated composition s. Also, the optical band gap values E_g^{opt}, were calculated from Wemple–Didomenico dispersion parameter E_o using the relation $E_{opt}^{WD} \approx E_o/2$ [16]. The obtained values agree w ith those determined by the other two methods as given in Table (1).

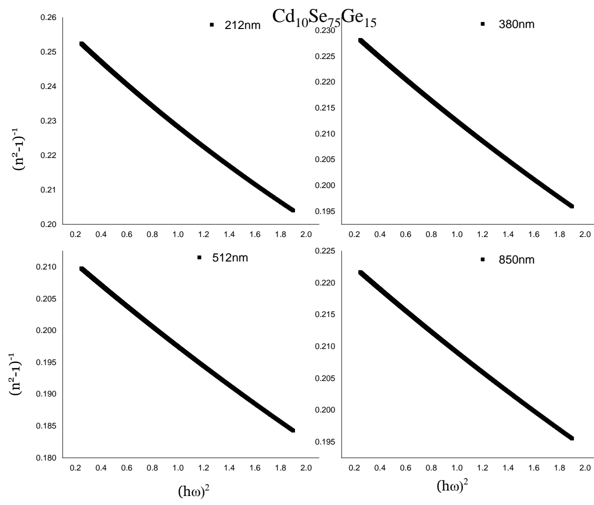

Fig.(8) A plot of $(n^2-1)^{-1}$ *against* $(h\nu)^2$ *for* $Cd_{10}Se_{75}Ge_{15}$ *amorphous films with different thicknesses.*

3.2.5. Determination of dielectric constant.

The obtained data of refractive index (n) can be analyzed to obtain the high frequency dielectric constant via two procedures[26]. ***The first procedure*** describes the contribution of the free carriers and the lattice vibrational modes of the dispersion. ***The second procedure***, however, is based upon the dispersion arising from the bound carriers in an empty lattice. To obtain a reliable value for the high-frequency dielectric constant (ε_∞),we employed both procedures.

(i) ***The first procedure***,

The following equation can be used to obtain the high frequency dielectric constant[26]

$$\varepsilon_1 = \varepsilon_{\infty(L)} - B\ \lambda^2 \qquad (4)$$

where ε_1 is the real part of dielectric constant, $\varepsilon_{\infty(L)}$ is the lattice dielectric constant, λ is the wavelength and B is given by ($e^2N / 4\pi^2\ \varepsilon_o\ m^*c^2$) where e is the charge of the electron, N is the free charge-carrier concentration, ε_o is the permittivity of free space, m^* the effective mass of the electron and c the velocity of light. It is observed that the dependence of $\varepsilon_1=n^2$ (in the transparent region k=0) on λ^2 is linear at longer wavelengths, as shown in Fig. (9). Extrapolating the linear part of this dependence to zero wavelengths gives the value of $\varepsilon_{\infty(L)}$ and from the slopes of these lines we can calculate the values of N/m^* for the investigated compositions. Values of $\varepsilon_{\infty(L)}$ and N/m^* are given in Table (3).

(ii) ***The second procedure***,

The high-frequency properties of the investigated films could be treated as a single oscillator of wavelength λ_o at high frequency by applying a simple classical dispersion relation [26]. If n_s is the refractive index of an empty lattice at infinite wavelength λ_o, it will vary as:

$$(n_s^2 - 1) / (n^2 - 1) = 1 - (\lambda_o/\lambda)^2 \qquad (5)$$

Where λ_o and n_s have been evaluated from plots of $(n^2 - 1)^{-1}$ against λ^{-2} given in Fig. (10). The values of n_s^2 can be calculated by extrapolating the obtained lines to the y-axis, while λ_o was calculated from the slopes of the linear part of the lines of Fig.(10) and equation (5). Values of $n_s^2 = \varepsilon_{\infty(s)}$ and λ_o are given in Table (3).

Values of $\varepsilon_{\infty(L)}$ and $\varepsilon_{\infty(s)}$ obtained by both procedures are agree with each other. The reason for this agreement, despite the difference in procedures used, is that the lattice-vibrations and plasma frequencies ω_p are well separated from the absorption band-edge frequency.

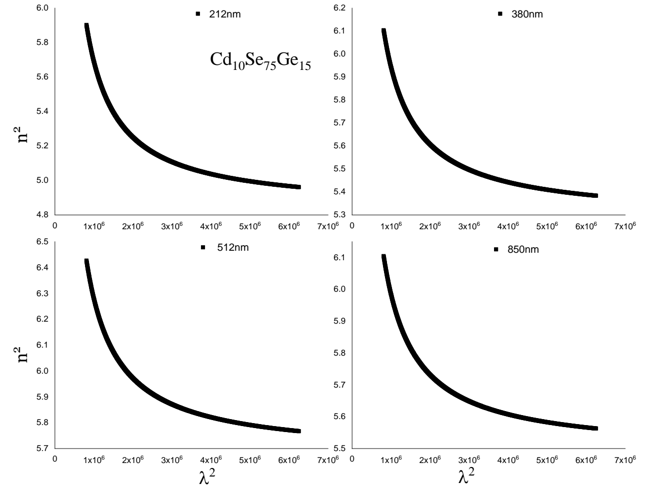

Fig.(9) *A plot of* ε_1 *as a function of* λ^2 *for* $Cd_{10}Se_{75}Ge_{15}$ *amorphous films with different thicknesses.*

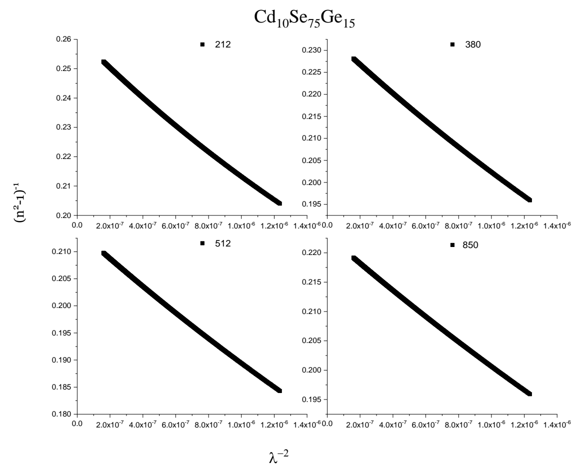

Fig.(10) *A plot of* $(n^2-1)^{-1}$ *against* λ^{-2} *for* $Cd_{10}Se_{75}Ge_{15}$ *amorphous films with different thicknesses.*

Table (3)

The parameters $\varepsilon_{\infty(L)}$, $\varepsilon_{\infty s}$, N/m^* , single oscillator of wav elength λ_o and plasma frequencies ω_p for $Cd_{10}Se_{75}Ge_{15}$ *amorphous films with different thicknesses.*

Compo sition	$\varepsilon_{\infty L}$	N/m^* ($m^{-3}.Kg^{-1}$)	λ_o (nm)	ω_p (s^{-1})	$\varepsilon_{\infty s}=n_s^2$
850nm	5. 9403	2.3×10^{56}	656	4.1×10^{14}	5.494
512nm	6.226	2.8×10^{56}	718	3.6×10^{14}	5.686
380nm	5.8837	3.1×10^{56}	807.9	1.23×10^{14}	5.297
212nm	5.6117	4.02×10^{56}	995	4.6×10^{14}	4. 86

The obtained values of the optical relative dielectric permi ttivity $\varepsilon_{\infty s} = n_o^2$ are in the same order with those obtained before [24,25,27] for the investigated films.

According to Penn's theory [28], which is applicable to ch alcogenide semiconductors, we have

$$n^2 = 1 + (h\ \omega_p / E_g^{opt})^2 \qquad (6)$$

where ω_p is the plasma frequency (a resonant frequency f or free oscillations of the electrons about their equilibrium positions), determined by the ratio

$$\omega_p^2 = e^2 N / \varepsilon_0\varepsilon_{\infty L}\ m^* \qquad (7)$$

Using our results of N / m^* given in Table 3, ω_p can be calculated from equation (8) and given also in the same T able.

3.2.6. Determination of the complex dielectric constant n ear the absorption edge.

The complex refractive index $\hat{n} = n + ik$ and complex dielectric constant $\hat{\varepsilon} = \varepsilon_1 + i\varepsilon_2$ characterize the optic al properties of any solid material. The real and imaginary parts of the dielectric constants ε_1 and ε_2 of the inves tigated films (in the absorption region) were also determin ed by the following relations [29]:

$$\varepsilon_1 = n^2 - k^2 = \varepsilon_\infty - \left(\frac{e^2 N}{4\pi^2 c^2 \varepsilon_o m^*}\right)\lambda^2, \qquad (8)$$

and

$$\varepsilon_2 = 2nk = \left(\frac{\varepsilon_\infty \omega_p^2}{8\pi^2 c^3 \tau}\right)\lambda^3, \qquad (9)$$

where ε_∞ is the high frequency dielectric constant, ω_p is the plasma frequency, τ the dielectric relaxation time and $k = \alpha\lambda/4\pi$. Values of ε_1 and ε_2 can be calculated as it is directly related to the density of states within the for bidden gap of the investigated compositions[40]. Variation of ε_1 and ε_2 with $h\nu$ are shown in Fig.(11) and (12) f or all investigated film compositions. It is seen that both ε_1 and ε_2 follow the same pattern and increase with incr easing photon energy and values of ε_1 are higher than th at of ε_2.

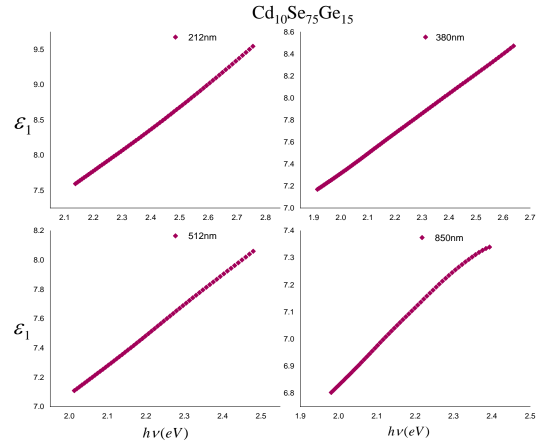

Fig.(11) *Plots of ε_1 as a function of $h\nu$ for the investig ated thin films.*

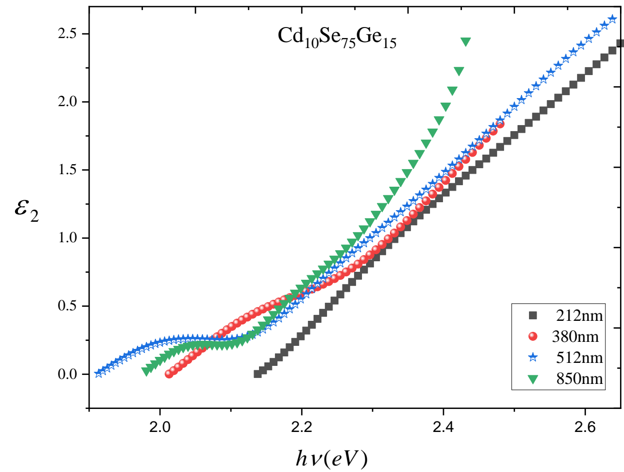

Fig.(12) *Plots of ε_2 as a function of $h\nu$ for the investi gated thin films.*

3.2.7. *Determination of the dissipation factor* $\tan\delta$.

The dissipation factor (loss tangent) $\tan\delta$ can be calcula ted according to the following equation [30]:

$$\tan\delta = \frac{\varepsilon_2}{\varepsilon_1}, \qquad (10)$$

The variation of the dissipation factor of the investigated f ilms with frequency ν is shown in Fig.(13). It is found t hat $\tan\delta$ increases with increasing frequency.

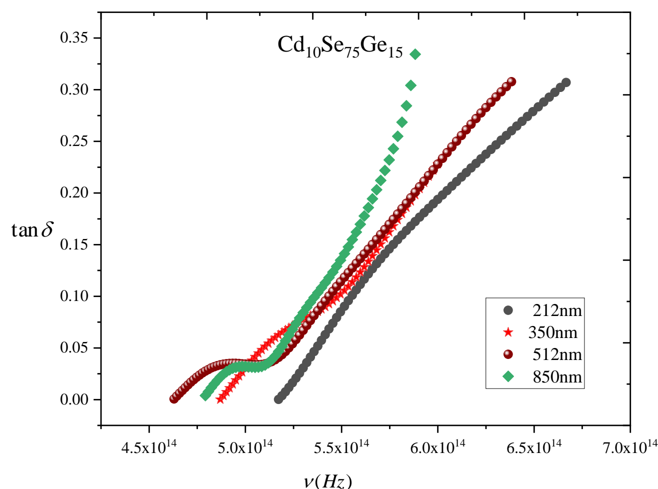

Fig.(13) *Dependence of the dissipation factor* $\tan\delta$ *on the frequency* ν *for the investigated thin films.*

4- Conclusions.

The refractive index n and absorption index k were com puted from the obtained $T(\lambda)$ using Swanepoel's method. The obtained values of the optical band gap E_g^{opt} calcu lated in terms of Tauc method and Wemple Didomenico model E_g^{WD} are in good agreement with each other. The t ype of optical transition responsible for optical absorption is indirect. It must be noticed that values of $\varepsilon_{\infty l}$ and $\varepsilon_{\infty s}$ obtained by two different procedures approximately agree with each other.

References

[1] S.A. Fayek, S.S. Fouad, Vacuum 52 (1999) 359.

[2]D.E. Carlson and C.R. Wronski, Appl. Phys. Lett., 28 (1976) 671.

[3]R.M. Mehra, A. Ganjoo and P.C. Mathur, J. Appl. Phys, 75 (1994) 7334.

[4]N.F. Mott, Phil. Mag., 19 (1969) 835.

[5]M. A. Mageed Khan, M. Zulfequar, M. Hussain, J. Phy s. Chem. Solids., 62(2001)1093.

[6] I Shu, Sharma, S K Tripathr, P. B. Barman, J. of phys. D: Appl. Physics 4(2007)4460.

[7] H.E Atyia, N.A. Hegab, M.A. Afifi , M.I. Ismad , J. Alloys and Comp. 574(2007)345.

[8] H.E Atyia , N.A. Hegab , Eur. Phy. J. Appl. Phys. 63 (2013)10301.

[9]M.F.A. Alias, M.N. Makadsi and Z.M. Al-Ajeli, Turk. J. phys., 27(2003)133.

[10]Y.L.A. El-Kady, Physica B 275(2000)344.

[11]M.M. Hafiz, A.A. Othman, M.M. Elnahass and A.T. Al-Motasem, Physica B 390(2007)286.

[12]H. El-Zahed and A. El-Korashy. Thin. Solid. Films . 3 76(2000)236.

[13]H.E. Atyia, Physica B 403(2008)16.

[14]S.A.Fayek and S.M.El-Sayed, NDT&E International 3 9(2006)39.

[15]R. Swanepoel, J. Phys. E: Sci. Instrum., 16 (1983) 12 14.

[16]E. Márquez, A.M. Bernal-Oliva, J.M. González-Leal, R. Prieto-Alcón, A. Ledesma, R. Jiménez-Garay, I. Mártil, Mater. Chem. Phys., 60 (1999) 231.

[17]J. Tauc, R. Grigorovici and A. Vancu, Phys. Status So lidi B 15 (1966) 627.

[18]F. Urbach, Phys. Rev., 92 (1953) 324.

[19]J. Olley, Solid State Commun., 13 (1973) 1437.

[20]M. Suzuki, H. Ohdaira, T. Matsumi, M. Kumeda and T. Shimizu, J. Appl. Phys., 16 (1977) 221.

[21]N.F. Mott and E.A. Davis, "Electronic Process in Non -Crystalline Materials", Clarendon Press, Oxford, (1971).

[22]M. Didomenico, S.H. Wemple, J. Appl. Phys., 40 (196 9) 720.

[23]S.H. Wemple, M. Didomenico, Phys. Rev. B, 3 (1971) 1338.

[24]K.M. Glassford, J. R. Chelikowsky, Phys. Rev. B, 4 6 (1992) 1284.

[25]N. El-Kabany, E.R. Shaaban, N. Afify and A.M. Abou -sehly, Physica B403(2008)31.

[26] J.N. Zemel, J.D. Jensen and R.B. Schoolar, Phys. Re v. A 140 (1965) 330.

[27]Ahmed S. Solieman, Mohamed M. Hafiz, Abdel-hami d A. Abu-Sehly & Abdelnaser A. Alfaqeer Journal of Tai bah University for Science 8 (2014) 282–288

[28]D. Minkov, E. Vateva, E. Skordeva, D. Arsova, M. Ni kiforova and G. Nadjakov, J. Non-Cryst. Solids 90 (1987) 481.

[29] M.M. Wakkad, E.Kh. Shokr, S.H. Mohamed, J. Non-Cryst. Solids, 265 (2000) 157.

[30] F. Yakuphanoglu, A. Cukurovali, İ. Yilmaz, Physica B, 351 (2004) 53.